Convergence of the Chirped Return-to-Zero and Dispersion Managed Soliton Modulation Formats in WDM Systems

R.-M. Mu and C. R. Menyuk, *Fellow, IEEE, Fellow, OSA*

***Abstract*—We investigated chirped return-to-zero (CRZ) and dispersion-managed soliton (DMS) formats that have been employed in experimental demonstration systems at Tyco [1], [2], CNET [3]–[5], and KDD [6]–[8]. We find that the DMS format and the CRZ pulse format used in these systems have been converging. By careful study of noise effects, single-channel nonlinear effects, and multichannel nonlinear effects, we provide evidence that these systems all operate in a quasi-linear region. In this regime, the pulse shape evolution is dominated by linear dispersion and the spread in the eye diagrams is dominated by signal-spontaneous beat noise, much as would be the case in a linear system. However, it is necessary to carefully manage the nonlinearity in these systems to minimize timing jitter due to interpulse interactions in a single channel, as well as interchannel interactions. Thus, nonlinearity plays an important role in system design.**

***Index Terms*—Amplified spontaneous emission (ASE) noise, chirped return-to-zero (CRZ), dispersion managed soliton (DMS), nonlinearity, quasi-linear, slope compensation, symmetric, wavelength division multiplexing (WDM).**

I. Introduction

THERE has been a long debate in the optical communications community as to whether a soliton modulation format or a nonsoliton modulation format such as nonreturn-to-zero (NRZ) is preferable for high-data-rate wavelength division multiplexed (WDM) communications. Over the last decade, as individual channel data rates and the number of WDM channels have continued to grow, both formats have evolved substantially. Solitons have evolved into dispersion managed solitons (DMS) and NRZ has evolved into chirped return-to-zero (CRZ). There are a number of successful laboratory testbed WDM systems that have been experimentally demonstrated. Among them is the system of Bergano *et al.* at Tyco [1], [2], referred by the authors as a CRZ system, that models a transoceanic link. Also among them is the system of Favre *et al.* [3] and Le Guen *et al.* [4], [5] at CNET, referred by the authors as a DMS system, that models a terrestrial link. In addition, the system of Taga *et al.* [6]–[8] at KDD, referred to as a return-to-zero (RZ) system, models a transoceanic link. These experimental systems have been described in recent Optical Fiber Communication Conference postdeadline sessions [1], [2], [4]–[6], articles in Electronics Letters [3], [7], and an article in the IEEE Journal of Quantum Electronics [8]. Thus, in some sense, they represent the experimental state-of-the-art, at the time they were presented, for laboratory demonstrations of high-data-rate WDM systems based on both soliton and nonsoliton formats.

It is our contention that the nonsoliton and soliton formats have effectively converged. The result is a new format that some call CRZ, some call DMS, and others simply call RZ. We reached this conclusion by developing simulation models that resemble the Tyco-CRZ, CNET-DMS, and KDD-RZ systems, and by comparing the pulse evolution and characteristics in these systems. In all three systems, one begins with raised-cosine pulses that are produced by a $LiNbO_3$ modulator. One then chirps the input pulse. In the Tyco-CRZ and KDD-RZ systems, this chirp is imposed by a $LiNbO_3$ phase modulator. In the CNET-DMS system, this chirp is imposed by a 3.5-km length of dispersion-compensating fiber (DCF) via the Kerr effect. The pulses then evolve along the transmission line. All three systems use dispersion maps in which the pulses stretch and shrink substantially in one period. In addition to that, however, we find that the pulse duration at the end point of each map period changed substantially along the fiber at most wavelengths. At the end of the transmission, the pulse duration is substantially smaller in all three systems than at the beginning. The relationship between the initial pulse duration, the final pulse duration, the initial chirp, and the average dispersion in the transmission line is almost exactly predicted by linear theory. The Kerr nonlinearity only plays a small role in the pulse evolutions at the powers at which pulses are transmitted in these three systems. This behavior contrasts strongly with the behavior in periodically stationary DMS systems like the ones studied by Suzuki *et al.* [9] and by Jacob *et al.* [10] in which the pulse returns to the same shape after every period in the dispersion map. Observation of the eye diagrams in all three systems shows that the noise-induced spread of the rails is dominated by spontaneous-signal beat noise, in contrast to the periodically stationary DMS systems, where the dominant noise effect is either timing jitter or exponentially growing noise in the spaces. For these reasons, we refer to all three test systems as quasi-linear.

By referring to these three systems as quasi-linear, we do not intend to imply that nonlinearity is unimportant. On the

Manuscript received May 7, 2001; revised December 20, 2001. This work was supported by the Air Force Office of Scientific Research, the Department of Energy, and the National Science Foundation.

R.-M. Mu is with the Department of Computer Science and Electrical Engineering, University of Maryland Baltimore County, Baltimore, MD 21250 USA, and also with Tycom Laboratories, Eatontown, NJ 07724 USA (e-mail: mu@umbc.edu).

C. R. Menyuk is with the Department of Computer Science and Electrical Engineering, University of Maryland Baltimore County, Baltimore, MD 21250 USA and also with PhotonEx Corporation, Maynard, MA 01754 USA.

Publisher Item Identifier S 0733-8724(02)02553-7.

contrary, nonlinearity plays a crucial role in all three systems, which are all designed to mitigate its effects. As one example, we may consider the Tyco-CRZ system. The dispersion in each of these channels is individually compensated. If nonlinearity were unimportant, then it would not matter whether this compensation occurred at the beginning of the transmission, the end of transmission, or both. In fact, this system suffers the least impairment when the compensation is split almost exactly between the beginning and the end of the transmission [11], [12]. We recently showed that nonlinear interpulse intrachannel interactions can lead to substantial timing jitter, much like in standard soliton systems, unless the compensation is split between the beginning and the end [13]. Although it is true, as stated earlier, that spontaneous-signal beat noise dominates the spread of the eye diagrams, it is also true that unless the nonlinearity is carefully mitigated, there is a large contribution from nonlinear timing jitter.

In presenting our comparison, we note that the parameters of our numerical models differ from the experiments in several ways. For example, the experimental Tyco-CRZ system uses orthogonal channel polarizations, a narrower channel spacing, and large-core fiber in their dispersion maps. The experimental CNET-DMS system interleaves pulses in orthogonal polarizations and achieves a data rate of 20 Gb/s by doing so. Details of the fiber, transmitter, amplifier, and receiver design are generally proprietary and, thus, unknown to us, and cannot be included in our models. These parameter choices do not affect our principal conclusion, which is that all three systems that we are modeling are quasi-linear. We have verified this point by changing the data rate per channel from 5 to 10 Gb/s, varying the channel spacing, changing the order and the bandwidth of the Bessel filter in our receiver model, and using fibers with $A_{\text{eff}} = 75\ \mu$m in studies of the Tyco-CRZ system [14]–[16]. At the same time, these parameter choices profoundly affect the performance of the systems and, in particular, how far it is possible to successfully propagate and detect signals. Thus, the model systems that we present in this paper should not be used to compare the relative performance of the experimental systems upon which our models are based.

In Section II, we present the numerical model that we use to compare our three model systems. In Section III, we outline the system configurations. In Section IV, we describe the evolution of a single typical channel. It is typical in the sense that the average dispersion in a single period of the dispersion map is not unusually close to zero, as would be required for the system to be periodically stationary. In Section V, we present full WDM studies. Finally, Section VI contains the conclusion.

II. Numerical Models

Our numerical system models are based on a variant of the nonlinear Schrödinger equation that we may write in the form [17]

$$i\frac{\partial q}{\partial z} + \frac{1}{2}\kappa(z)\frac{\partial^2 q}{\partial t^2} + \frac{i}{6}d\frac{\partial^3 q}{\partial t^3} + |q|^2 q = ia(z)q + \hat{F}(z,t). \quad (1)$$

Here, the pulse envelope q is normalized as $q = E(n_2\omega_0 L_D/A_{\text{eff}}c)^{1/2}$ where E is the electric field envelope, $n_2 = 2.6 \times 10^{-16}$ cm$^2/W$ is the Kerr coefficient, ω_0 is the central frequency, A_{eff} is the effective area, and c is the speed of light. The quantity L_D is the characteristic dispersion length; it equals $T_0^2/|\beta_0''|$ where T_0 is a characteristic time scale and β_0'' is a characteristic dispersion. The distance z is normalized as $z = Z/L_D$ where Z is the physical distance. The retarded time t is normalized as $t = (T - \beta_0' Z)/T_0$ where T is the physical time and β_0' is the inverse group velocity. Other quantities are normalized as $\kappa(z) = -\beta''(z)/|\beta_0''|$ and $d = -\beta_0''' T_0/|\beta_0''|$, where β_0''' is the third-order dispersion.

The average dispersion over a single map period is defined as $\bar{D} = (D_1L_1 + D_2L_2)/(L_1 + L_2)$ and $\bar{\beta}'' = (\beta_1''L_1 + \beta_2''L_2)/(L_1 + L_2)$ where D_1 or β_1'' is the dispersion of fiber segment 1 with the length of L_1, and D_2 or β_2'' corresponds to the dispersion of fiber segment 2 with a length of L_2. The distinction between the D_j and β_j'' is that the former are measured in units of ps/nm-km and are negative for normal dispersion, whereas the latter are measured in ps^2/km and are positive for normal dispersion. The residual average dispersion over the transmission distance L_T is given by $\delta\bar{D} = \int_0^{L_T} D(z)dz/L_T$ and $\delta\bar{\beta}'' = \int_0^{L_T} \beta''(z)dz/L_T$. Thus, we can define the effective dispersion length as $L_{D,\text{eff}} = T_{\min}^2/|\bar{\beta}''|$, where $T_{\min}$ is the minimum pulse duration at the end of the transmission line. We also define the effective nonlinear scale length as $L_{\text{NL,eff}} = 1/(\gamma\bar{P}_0)$ with the path average pulse peak intensity $\bar{P}_0 = \int_0^{L_T} P_0(z)dz/L_T$, whereas the variable $P_0(z)$ corresponds to the z-varying peak power of the pulse along the transmission line. We characterize all three model systems using the dimentionless quantities $\gamma_{\text{NL}} = L_T/L_{\text{NL,eff}}$ and $\gamma_D = L_T/L_{D,\text{eff}}$ [18], which allow us to compare the transmission length to the nonlinear scale length and dispersion scale length. These normalized quantities are comparable for all model systems, even though L_T is much shorter in the CNET-DMS system than in either the Tyco-CRZ or the KDD-RZ system, because the former system models terrestrial systems, whereas the latter system models transoceanic systems.

The variable $a(z) = \alpha(z)/2L_D$ where $\alpha(z)$ is the power gain or loss. The autocorrelation function for the Langevin term in (1) may be written as

$$\left\langle \hat{F}(z,t)\hat{F}^*(z',t')\right\rangle = 2\theta(z)G(z)\frac{n_2\hbar\omega_0^2 L_D}{A_{\text{eff}}T_0 c} \cdot\delta(z-z')\,\delta(t-t') \quad (2)$$

where $\hbar$ is the Planck's constant and $\theta(z)$ equals the spontaneous emission factor n_{sp} at the amplifiers and is zero elsewhere. The quantity $G(z)$ is the amplifier gain. In our models of the Tyco-CRZ and CNET-DMS systems, we use linear gain; however, in our model of the KDD-RZ system, we must include the gain saturation model in order to accurately calculate the pulse evolution and the amplified spontaneous emission (ASE) noise contribution. The reason for this distinction is that the KDD-RZ system includes inline spectral filtering of the individual channels, so that it is not possible to determine the exact gain necessary to compensate for the fiber loss *a priori*. By contrast, in the Tyco-CRZ and CNET-DMS systems, there is no inline filtering and we set the amplifier gain to exactly compen-

sate for the fiber loss. The gain saturation model was described in detail previously [17]. We solve (1) using a standard split-step approach.

The evaluation of the system performance will focus on determining the timing jitter and amplitude jitter. We will include ASE noise using the Monte Carlo method [17]. To calculate the timing jitter, we first define the central pulse time position t_p [19] as

$$t_p = \frac{1}{U}\int_{-\infty}^{\infty} t\,|q(t)|^2\,dt \tag{3}$$

where $U = \int_{-\infty}^{\infty} |q(t)|^2\,dt$ is the pulse energy. We next define the timing jitter as

$$\delta t = \left[\langle t_p^2\rangle - \langle t_p\rangle^2\right]^{1/2}. \tag{4}$$

The simulations include a square-law detector and an electrical fifth-order Bessel low-pass filter to model the receiver. For all of the cases discussed in this paper, the 3-dB bandwidth of this electrical filter is 8 GHz. The amplitude jitter is evaluated using a Q factor that is calculated from the electrical current at the receiver, with $Q = (\mu_1 - \mu_0)/(\sigma_1 + \sigma_1)$ where, as usual, the variables μ_1 and μ_0 are the means of the marks and the spaces, and σ_1 and σ_0 are the standard deviations of the marks and spaces. We set the following two conditions as the criteria for an acceptable system performance: 1) $Q \geq 6$ corresponding to a bit error ratio (BER) induced by the amplitude jitter less than 10^{-9}; and 2) $\delta t \leq 5.8$ ps corresponding to a BER induced by the timing jitter less than 10^{-9} with a detection window of 50 ps.

III. Schematic Configurations of the Tyco-CRZ, CNET-DMS, and KDD-RZ Systems

Based on the experimental reports [1]–[8], [20] as well as optimization in our own simulations, we developed simulation models that are intended to model as closely as feasible the three systems that we are comparing.

In our models of the Tyco-CRZ and KDD-RZ systems, we used initial pulses with a raised-cosine shape driven by a sinusoidal voltage and a cosinusoidal pulse modulation, described by the expressions

$$q = \sqrt{\frac{q_0}{2}\left\{1 + \cos\left[B\pi\sin(\Omega t)\right]\right\}} \tag{5}$$

$$\phi = A\pi\cos(\Omega t) \tag{6}$$

where, in (5), the variable q_0 is the initial pulse intensity and the variable B is the modulation index of the voltage driver that can be adjusted such that one can change the initial full-width at half-maximum (FWHM) duration. In the Tyco-CRZ system, we set B equal to 1.0, corresponding to an initial input pulse with an FWHM duration of 32 ps, whereas in the KDD-RZ system, we chose $B = 0.7$, corresponding to an initial input pulse with an FWHM duration of 50 ps. In (6), the quantity A is the phase modulation depth, Ω is the bit rate of the signal (10 Gb/s), and t is the time measured from the center of the bit window. The corresponding input chirp C is given by $C = \pi A\Omega^2$. In the simulation of CNET system, we launched the initial pulse shape described by (5) and we also set B equal to 1 so that the initial pulse has a narrower FWHM pulse duration, which we verified is the optimal launching condition. We used a piece of DCF instead of a phase modulator to chirp the initial signal. The corresponding input chirp C is determined by solving (1) in the prechirping DCF and then computing the negative of the second derivative of the phase at the center of the bit window.

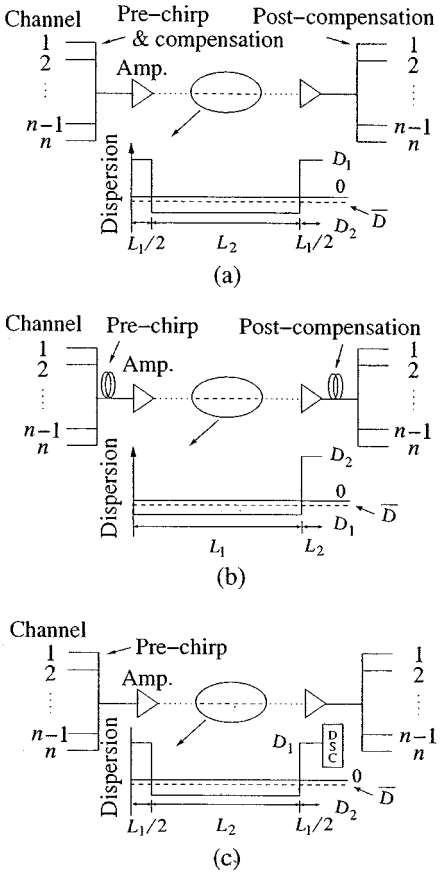

Fig. 1. Schematic configuration of the three WDM model transmission systems. (a) Tyco-CRZ system. (b) CNET-DMS system. (c) KDD-RZ system.

We show a schematic illustration of each of our three model system in Fig. 1.

A. Tyco-CRZ Model

As shown in Fig. 1(a), the dispersion map that we used to model the Tyco-CRZ system has one segment of length $L_1 = 160$ km with $D_1 = -2.125$ ps/nm-km and a second segment of length $L_2 = 20$ km with $D_2 = 17$ ps/nm-km at 1550 nm, corresponding to the point at which the average dispersion over the map period is zero. The amplifier spacing is 45 km and the total propagation distance is 5040 km. For both types of fibers, we assume a dispersion slope $dD/d\lambda = 0.075$ ps/nm^2-km, as well as an effective area $A_{\text{eff}} = 50\,\mu$m^2. The fiber loss is 0.21 dB/km and the spontaneous emission factor is $n_{\text{sp}} = 2.0$. These parameters correspond to the experiments of Bergano *et al.* [1], [2], except that the dispersion map period is smaller and we used no large effective area fiber. We chose a smaller period so that the dispersion management strength parameter γ_{map} corresponds to the value at which simulation studies showed the largest margin

[21]. We chose a phase modulation depth $A = -0.6$ for the initial chirp and an average power of 0.3 mW per channel at the input, assuming an equal number of marks and spaces. We found that this choice of average power is nearly optimal [16]. We computed the average power by dividing the total optical power over the entire computation time window. We compensate for the dispersion symmetrically, which, as noted earlier, is the optimal choice [13]. The path average pulse peak intensity $\bar{P}_0$ equals 0.24 mW in this model system where $\gamma = 2.11 \times 10^{-3}$ m^{-1}W^{-1}. Hence, the effective nonlinear length $L_{\mathrm{NL,\,eff}} = 1/(\gamma P_0)$ in this system is about 1960 km so that $\gamma_{\mathrm{NL}} = 2.6$. The minimum pulse duration at the end of the transmission is 21 ps in a channel that is offset -4.8 nm from the zero dispersion wavelength. For this channel, we find $\bar{\beta}'' = 0.462$ ps^2/km and we find a pulse spreading during transmission that is typical of most channels. We then find that dispersion length $L_{D,\,\mathrm{eff}} = 960$ km, so that $\gamma_D = 5.3$.

B. CNET-DMS Model

In our model of the CNET-DMS system, shown in Fig. 1(b), the map period is 120-km long and consists of a long span of standard single-mode fiber (SMF) with a dispersion D_1 of 16.4 ps/nm-km at 1550 nm and a length L_1 of 102 km, followed by a shorter span of DCF with a dispersion D_2 of -95 ps/nm-km at 1550 nm and a length L_2 of 17.3 km. The dispersion slope of the SMF is 0.075 ps/nm^2-km, whereas the dispersion slope of the DCF is -0.2 ps/nm^2-km, which balances the dispersion and the dispersion slope of the SMF simultaneously. The A_{eff} of the SMF is 50 μm^2 and the fiber loss is 0.2 dB/km, whereas $A_{\mathrm{eff}} = 20$ μm^2 with a fiber loss of 0.6 dB/km in the DCF segments. The average dispersion $\bar{D}$ is about 0.25 ps/nm-km with an average dispersion slope of 0.035 ps/nm^2-km. In each period of the map, there is one amplifier following the SMF span and another one following the DCF span with $n_{\mathrm{sp}} = 2.0$ in both amplifiers. The gain of the first amplifier $G_1 = 15.42$ dB, while the gain of the second amplifier $G_2 = 16.38$ dB, yielding the minimum ASE noise accumulation during this dual-stage amplification. The total transmission distance is 1431.6 km. Because the dispersion slope is reduced by using DCF with a negative dispersion slope, the signals carried by all the wavelengths could be prechirped by propagation through a single 3.5-km-long section of DCF (pre-DCF) with the dispersion of -100 ps/nm-km at 1550 nm and the dispersion slope of -0.2 ps/nm^2-km. The fiber loss is 0.5 dB/km with A_{eff} equal to 20 μm^2. The residual dispersion over the entire transmission line was adjusted by a piece of SMF fiber at the end of the transmission (post-SMF), whose length was chosen to maximize the pulse compression at the end, leading to a residual dispersion $\delta\bar{D}$ of approximately 0.034 ps/nm-km at the 1550 nm. This CNET-DMS model resembles the experimental system of Le Guen *et al.* [5]. The typical average power in a WDM channel at the beginning of the transmission line is 1.2 mW. Just as in the Tyco-CRZ model, we numerically calculated the effective nonlinear length $L_{\mathrm{NL,\,eff}} = 364$ km with $\bar{P}_0 = 1.3$ mW and the effective dispersion length $L_{D,\,\mathrm{eff}} = 610$ km with $T_{\min} = 14$ ps, so that $\gamma_{\mathrm{NL}} = 3.9$ and $\gamma_D = 2.3$, respectively.

C. KDD-RZ Model

Our model of the KDD-RZ system, shown in Fig. 1(c), contains a 1033-km-long dispersion shifted fiber (DSF) segment with $D_2 = -1.694$ ps/nm-km at 1550 nm. Before and after the DSF fiber segment, there is a segment of SMF with length $L_1/2$ of 50 km and a dispersion D_1 of 17.5 ps/nm-km at 1550 nm. Hence, the path average dispersion is zero at 1550 nm. The average dispersion slope is 0.07 ps/nm-km in both the SMF and DSF segments. There are 20 amplifiers in the DSF segment equally spaced 51.65 km apart with $n_{\mathrm{sp}} = 1.2$. We also placed amplifiers immediately after the segments of SMF that come before and after the DSF segment. Our arrangement differs somewhat from the original KDD arrangement, in which the second SMF was put in the middle of the DSF span [6], [7]. We observed that we can achieve larger tolerance of the input pulse conditions, less oscillation of the pulse duration along the propagation, and a slightly larger dispersion compensation tolerance by choosing our arrangement. In order to achieve an error-free WDM transmission over 9064 km, we used fibers with a large effective area $A_{\mathrm{eff}} = 75$ μm^2 in both segments of the map. In an earlier study, we demonstrated that a fiber with a large effective area can significantly improve the eye degradation due to the nonlinear interactions [16]. The fiber loss is 0.21 dB/km. As in the Tyco-CRZ system shown in Fig. 1(a), there are individual phase modulators at the beginning of the transmission to prechirp the signal at each channel. Moreover, we also include a dispersion slope compensator (DSC) in each loop period, as was done in the experimental demonstrations [6], [7]. A twenty-third amplifier was employed after the DSC module to compensate for the loss due to the DSC. Inside the DSC module, there are a pair of flat-top array waveguide gratings acting as a multiplexer (MUX) and demultiplexer (DEMUX) pair with a 3-dB bandwidth of 0.5 nm, as well as a 1-dB bandwidth of 0.3 nm. The DEMUX separates channels before the individual dispersion compensation and the MUX combines channels after the dispersion compensation. In the simulation, we include the effect of the array waveguide gratings by introducing a lumped filter. The filter function is

$$H(\omega) = \sqrt{H_0}\exp\left[-\frac{1}{2\ln 2}\left(\frac{2\omega}{\omega_B}\right)^4\right] \tag{7}$$

where the coefficient H_0 corresponds to the insertion loss and ω_B corresponds to the 3-dB bandwidth. The loss of each array waveguide grating is 5 dB. Each individual channel has a 5-km-long independent dispersion compensation fiber of followed by an erbium-doped fiber amplifier (EDFA) to compensate for the loss of this dispersion compensation fiber and a 2-nm optical Gaussian filter to eliminate the ASE noise accumulation. The dispersion of the compensating fiber inside the DSC can be calculated individually according to the initial chirp. For a WDM channel that is offset by -2.0 nm from the zero dispersion wavelength, we chose a residual average dispersion $\delta\bar{D} = -0.028$ ps/nm-km, corresponding to the initial modulation depth $A = -0.4$. We set the unsaturated gain coefficient of the first 22 EDFAs $G_{1\ldots22,\,0}$ equal to 12.25 dB and the unsaturated gain of the last EDFA in the loop $G_{23,\,0}$

TABLE I
FIBER PARAMETERS IN (A) TYCO-CRZ SYSTEM, (B) CNET-DMS SYSTEM, AND (C) KDD-RZ SYSTEM

	fiber	D (ps/nm-km)	D' (ps/nm^2-km)	L (km)	A_{eff} (μm^2)	$n_2 \times 10^{-16}$ (cm^2/W)	α (dB/km)
(a)	SMF	17	0.075	20	50	2.6	0.21
	DSF	−2.125	0.075	160	50	2.6	0.21
(b)	SMF	16.4	0.075	102	50	2.6	0.21
	DCF	−95	−0.2	17.5	20	2.55	0.6
	Pre-DCF	−100	−0.2	3.5	20	2.55	0.5
	Post-SMF	16.4	0.075	2.9	50	2.6	0.21
(c)	SMF	17.5	0.07	100	75	2.55	0.21
	DSF	−1.694	0.07	1033	75	2.6	0.21

TABLE II
FIBER PARAMETERS IN (A) TYCO-CRZ SYSTEM, (B) CNET-DMS SYSTEM, AND (C) KDD-RZ SYSTEM FOR A TYPICAL CHANNEL SELECTED IN THE SINGLE CHANNEL STUDIES

	fiber	D (ps/nm-km)	β'' (ps^2/km)	$\overline{D}$ (ps/nm-km)	$\overline{\beta}''$ (ps^2/km)	$\delta\overline{D}$ (ps/nm-km)	$\delta\overline{\beta}''$ (ps^2/km)	A
(a)	SMF	16.64	−21.33	−0.36	0.462	−0.028	0.036	−0.6
	DSF	−2.485	3.186					
(b)	SMF	16.4	−21.03	0.246	−0.315	0.034	−0.044	
	DSF	−95	121.79					
(c)	SMF	−1.824	2.351	−0.14	0.179	−0.028	0.036	−0.4
	DSF	17.36	−22.256					

equal to 13 dB so that the average power in each WDM channel is about 0.44 mW. Consequently, the effective nonlinear length $L_{\text{NL, eff}} = 3140$ km with $\bar{P}_0 = 0.23$ mW and the nonlinear coefficient $\gamma = 1.4 \times 10^{-3}$ m^{-1}W^{-1}. The effective dispersion length L_D is 2290 km with $T_{\text{min}} = 24$ ps at the WDM channel has already been described. Thus, we obtain $\gamma_{\text{NL}} = 2.9$ and $\gamma_D = 4.0$.

Comparing the parameters of our three model systems, we find that the power in the CNET-DMS system is approximately four times greater than in our model of the Tyco-CRZ system, but the total propagation length is approximately three to four times smaller. In our model of the KDD-RZ system, the power is about the same as in our model of the Tyco-CRZ system; however, we used a large effective area fiber that has a reduced nonlinear coefficient by a factor of 1.5. Consequently, we found that the values of γ_{NL} are all within a factor of two of each other. The same is true for γ_D. We summarize the fiber parameters in all three model systems in Table I.

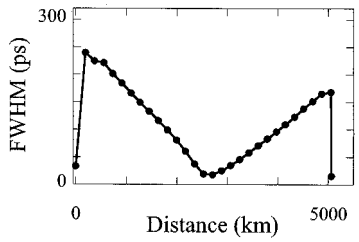

Fig. 2. Evolution of the FWHM pulse duration at the end of each map period in the Tyco-CRZ system.

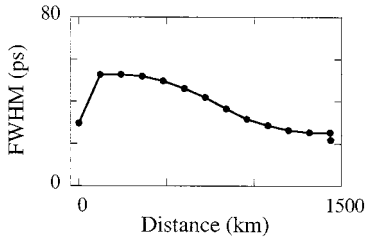

Fig. 3. Evolution of the FWHM pulse duration at the end of each map period in the CNET-CRZ system.

IV. INTRACHANNEL SYSTEM BEHAVIOR

We begin our study by focusing on the single-channel signal propagation, which allows us to explore a wider parameter space and to better understand the pulse evolution and characteristics in our three model systems. We will describe a case in which the average dispersion in the transmission line differs from zero by an amount that is typical for most channels in a WDM system and allows us to discuss the dynamics of the dispersion compensation. In our model of the Tyco-CRZ system, we offset the channel wavelength from the zero dispersion point by −4.8 nm, whereas for the KDD-RZ system, we offset the channel wavelength from the zero dispersion point by −2.0 nm. In our model of the CNET-DMS system, we do not offset the wavelength, because the dispersion at the center wavelength already differs significantly from zero. Meanwhile, the better compensation of the third-order dispersion implies that an offset is unnecessary. We list the fiber parameters for the particular channels that we chose in the three model systems in Table II.

We show the evolution of the FWHM of a single pulse at the end of each map period along the transmission line for each of our three model systems in Figs. 2–4. In each of these three model systems, the final pulse is compressed relative to the initial pulse by a factor of 1.5 to 2. However, the intermediate evolution is quite different in all three cases. In our model of the Tyco-CRZ system, shown in Fig. 2, the chirped pulse first stretches by six to seven times its initial duration. During the

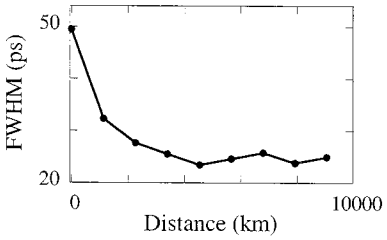

Fig. 4. Evolution of the FWHM pulse duration at the end of each map period in the KDD-RZ system.

propagation, the residual dispersion in the transmission, combined with the initial chirp, leads to a gradual pulse compression until the pulse reaches its minimum duration at the midpoint of the propagation. Then, the pulse stretches again until it resumes a pulse duration of two to three times the original duration before the final compression in the compensating fiber. We note that this gradual change in the pulse duration occurs in addition to the far more rapid change inside the dispersion map. The pulse expansion is large in our model of the Tyco-CRZ system because the compensation is only done at the beginning and the end of the transmission line. By contrast, the CNET-DMS system uses inline DCFs that nearly compensate both the dispersion and the dispersion slope in every map period along the line, although the remaining dispersion is still sizeable, which minimizes interchannel interactions. The initial stretch is produced by dispersion in the prechirp DCF. Moreover, the chirp that is produced by the prechirp DCF fiber is smaller than what is produced by phase modulation. The pulses only stretch a little under twice their initial pulse duration and then gradually compress during the remaining propagation to their final pulse duration shown in Fig. 3. In the KDD-RZ system seen in Fig. 4, the dispersion is compressed in every 1000-km-long loop period. In this case, the pulse compresses continually during its propagation through the system with most of the compression occurring in the first couple of periods of the dispersion map. Imperfect compression, along with a residual chirp, leads to small oscillations in the pulse duration at the end of the pulse propagation.

Despite the large differences in the evolution of the three model systems, there is one important similarity that is clearly visible. All three systems use an initial chirp, in combination with the residual dispersion, to compress the pulse at the end. One can better understand the pulse compression by comparing the observed behavior to the linear propagation of a Gaussian-shape pulse [16]. This theory predicts that the output pulse duration $T_{\rm out}$ at a distance $z = Z$ is related to the input pulse duration $T_{\rm in}$ through the relation

$$\frac{T_{\rm out}}{T_{\rm in}} = \left[\left(1+\frac{c_0\delta\bar{\beta}''Z}{T_{\rm in}^2}\right)^2 + \left(\frac{\delta\bar{\beta}''Z}{T_{\rm in}^2}\right)^2\right]^{1/2} \tag{8}$$

where we let $c_0 = CT_{\rm in}^2 = \pi A\Omega^2 T_{\rm in}^2$, C is the chirp parameter, A is the modulation depth, $\Omega/2\pi$ is the bit rate, and we recall that $\delta\bar{\beta}''$ is the residual average dispersion. One can see that when $\delta\bar{\beta}''c_0 < 0$, the pulse will initially compress. In this case,

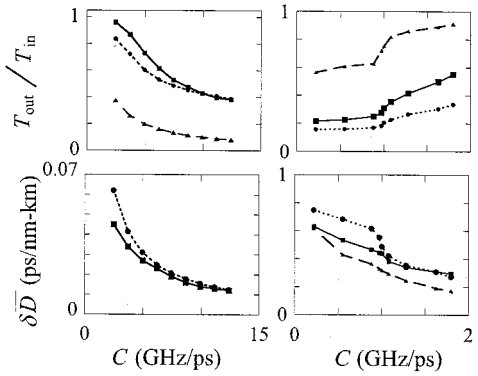

Fig. 5. Dependence on the chirp C of the pulse compression ratio $T_{\rm out}/T_{\rm in}$ and the optimal residual average dispersion $\delta\bar{D}$. The short dashed lines with filled circles are the results predicted by modified linear theory and the solid lines with squares represent the result of the full nonlinear model, whereas the long dashed lines with triangles represent the prediction from Gaussian theory. The left side corresponds to the results in the Tyco-CRZ system, whereas the right side represents the results in the CNET-DMS system. We do not show the Gaussian theory in the dependence of the chirp versus the optimal residual average dispersion in the Tyco-CRZ system (the left lower figure) because there is no visible difference between the Gaussian theory and the modified linear theory.

the minimal pulse duration $T_{\rm min}$ occurs at $Z = Z_{\rm min}$ and their values are given by

$$Z_{\rm min}\delta\bar{\beta}'' = -\frac{c_0}{1+c_0^2}T_{\rm in}^2 \tag{9}$$

$$\frac{T_{\rm min}}{T_{\rm in}} = \frac{1}{(1+c_0^2)^{1/2}}. \tag{10}$$

We have compared the predictions of this simple linear theory to the optimized evolution in our three model systems. We have also compared a modified linear theory in which we solve the propagation equation (1), with the same initial conditions as in the complete theory, but with the Kerr nonlinearity turned off. We show the results of this comparison in Fig. 5 for our models of the Tyco-CRZ and CNET-DMS systems. There is no visible distinction between the Gaussian theory and the modified linear theory in the dependence of the chirp versus the optimal residual dispersion in the Tyco-CRZ system; thus, the former curve does not appear. We see that the Gaussian approximation is qualitatively useful, but it is not quantitatively exact in most cases. By contrast, the modified linear theory predicts output pulse durations for our model of the Tyco-CRZ model system that agree with the prediction of the full nonlinear theory within 10% to 15%. In the CNET-DMS model system, the pulses are less chirped and are compensated each period; thus, the discrepancies are somewhat larger. We have not included the KDD-RZ system in Fig. 5 because stable pulses only exist for a limited range of the chirp parameters -5.2 GHz/ps $< C < -3.7$ GHz/ps. Within this range, the residual average dispersion $\delta\bar{D}$ only varies between -0.03 ps/nm-km and -0.02 ps/nm-km, correspondingly, and the ratio $T_{\rm out}/T_{\rm in}$ varies between 0.53 and 0.67. These ranges are limited by the strong filtering that occurs due to cascading the narrow band MUX and DEMUX elements in the DSCs. We found that when $A = -0.4$, corresponding to

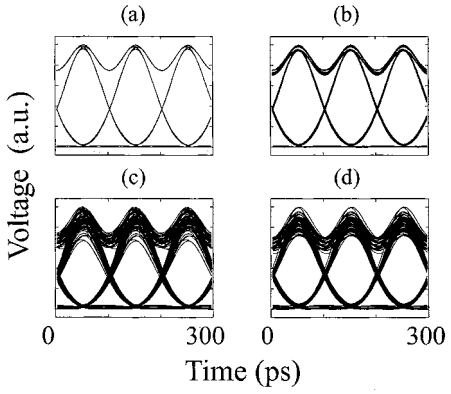

Fig. 6. Eye diagrams in a single channel case in the Tyco-CRZ system. (a) The case in which neither nonlinearity nor ASE noise is included in (1). (b) The case in which we only neglect the ASE noise. (c) The case in which we only neglect the nonlinearity in the simulations. (d) The case in which neither nonlinearity nor ASE is neglected.

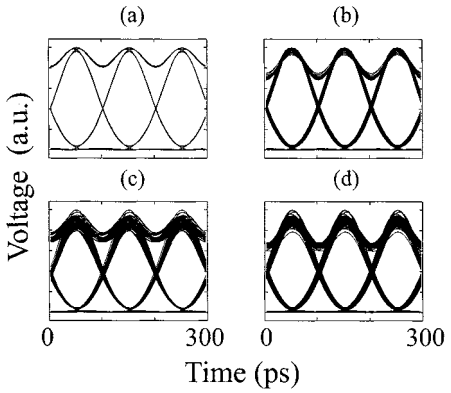

Fig. 7. Eye diagrams in a single channel case in the CNET-DMS system, where (a)–(d) are the same as in Fig. 6.

$C = 4.96$ GHz/ps, the values of $\delta\bar{D}$ and the ratio of $T_{\rm out}/T_{\rm in}$ predicted by the full nonlinear model are -0.028 ps/nm-km and 0.53, by the modified linear model are -0.023 ps/nm-km and 0.51, and by the Gaussian model are -0.038 ps/nm-km and 0.2. The discrepancy between the full nonlinear theory and the modified linear theory is only 20%.

We now turn from an examination of single-pulse propagation to examination of a complete channel consisting of a 64-bit pseudorandom bit stream. Using the same parameters as in Figs. 2–4, we show the electrical eye diagrams for all three systems in Figs. 6–8 that are calculated using our receiver model. In order to determine the principal source of the impairments, we sequentially turn off both the ASE noise and the nonlinearity, just the ASE noise, just the nonlinearity, and neither ASE noise nor nonlinearity. In our models of the Tyco-CRZ system and the CNET-DMS system, the spontaneous-signal beat noise clearly dominates the impairments. In our model of the KDD-RZ system, nonlinearity does strongly impact the eye diagrams. However, the impairments in the center of the bit window, where the detection takes place, is dominated by signal-spontaneous beat noise.

We conclude that in all three model systems, the behavior resembles linear systems in two important respects. First, the pulse dynamics is dominated by the linear dispersion and the initial chirp. The nonlinearity plays a relatively small role in the single-pulse dynamics. Second, signal-spontaneous beat noise dominates the growth of impairments in the electrical eye diagrams. This behavior is typical for linear systems. At the same time, nonlinearity plays an important role in all three model systems. In particular, as mentioned previously, we have shown that unless dispersion compensation is divided between the beginning and the end of the transmission in the Tyco-CRZ system, the eye diagrams exhibit substantial timing jitter [13]. In other words, a property that is typical of linear system—that the spread in the eye diagrams is dominated by spontaneous-signal beat noise—does not hold unless the nonlinearity is properly mitigated. Thus, we refer to these systems as quasi-linear to indicate that they behave as if they were linear in important respects, but that nonlinearity and its mitigation play important roles.

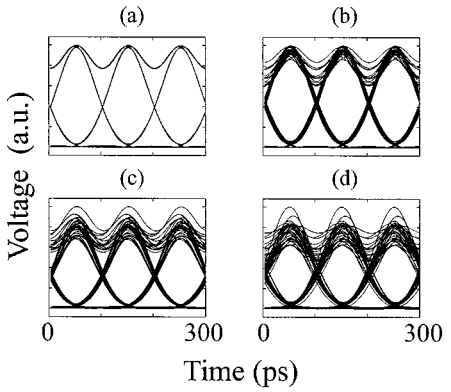

Fig. 8. Eye diagrams in a single channel case in the KDD-RZ system, where (a)–(d) are the same as in Fig. 6.

V. WDM Studies

In this section, we will study the performance of our three model systems with WDM. We keep seven or eight channels in our studies, which previous work indicates is sufficient to study the channel interactions in a full WDM system [22]. Channels that are far away do not affect each other much because they pass through each other quickly, due to dispersion. In the WDM systems that we modeled, the channels are evenly spaced in wavelength and each wavelength has a slightly different average dispersion. In all of our WDM simulations, we assumed that the EDFA has the same gain for all the WDM channels. In reality, an accumulated gain difference must be avoided by using passive gain-equalizing filters [23], [24].

Comparing the results of this section to those of the previous sections allows us to determine the importance of the interchannel interference and to verify that the pulse behaviors that we observed in our single-channel studies are not significantly altered by interchannel interactions. We kept seven channels in our models of the Tyco-CRZ and CNET-DMS systems and we kept eight channels in our models of the KDD-RZ system. We used the same system parameters as in Section III. The channel spacing in our models of the Tyco-CRZ and CNET-DMS systems is 0.6 nm, whereas in our model of the KDD-RZ system, it is 0.8 nm. In our model of the Tyco-CRZ system, we placed channel 4 at the zero average dispersion wavelength, which is 1550 nm; in our model of the CNET-DMS system, we placed

TABLE III
THE RESIDUAL DISPERSION IN THE EIGHT WDM CHANNELS OF THE KDD-RZ SYSTEM, WHERE CH = CHANNEL

Ch.	A	$\delta\overline{D}$ (ps/nm-km)	$\delta\overline{\beta}''$ (ps^2/km)
1	−0.4	−0.033	0.042
2	−0.4	−0.028	0.036
3	−0.4	−0.024	0.031
4	−0.4	−0.020	0.026
5	−0.4	−0.023	0.029
6	−0.4	−0.018	0.023
7	−0.4	−0.013	0.017
8	−0.4	−0.018	0.023

channel 4 at 1550 nm; however, the corresponding dispersion significantly deviates from zero. In our model of the KDD-RZ system, we place channels symmetrically around the central wavelength of 1550 nm and the zero dispersion occurs in between channels 4 and 5. The channel spacing in our model of the Tyco-CRZ model system is larger than in the experimental systems, but we did not use orthogonal polarizations in neighboring channels or forward error correction coding. In our model of the CNET-DMS model system, we use a bit rate of 10 Gb/s instead of 20 Gb/s, but we did not use orthogonal polarizations in neighboring bits to generate a 20-Gb/s pulse train. We applied the same prechirping and the same residual dispersion for all seven channels in our model of the Tyco-CRZ system. We fixed the length of the pre- and postcompensation fibers at 10 km for all seven channels, but we varied the fiber dispersion to obtain the optimal average dispersion. In the experimental system, one must vary both the fiber type and the length to obtain the optimal average dispersion. However, we have verified that as long as the accumulated dispersion in the pre- and postcompensation fibers are correct, the result does not change. In our model of the CNET-DMS system, there is no individual prechirp and postcompensation for each channel. Because the dispersion slope is small at the end of each map period, it is possible to use one piece of fiber to prechirp the pulse in all of the channels and, at the end, to use one postcompensation fiber to recover the pulse in all of the channels. In our model of the KDD-RZ system, we used the same chirp for all eight channels, but the residual dispersion after one loop period differs slightly from channel to channel, as shown in Table III. We fixed the length of compensating fiber at 5 km but varied the fiber dispersion to obtain the optimal residual average dispersion.

The simulation results for the input and output spectra are shown in Figs. 9–11. We note that the spectra are the same for all of the channels in each case within the resolution of the plot. There is a tendency for the spectral intensity to decrease in between the channels in the KDD-RZ transmission system due to the cascading of the DSC, which includes a MUX and DEMUX pair that gradually narrows the signal spectrum. In Figs. 12–14, we showed the eye diagrams at the receivers in these systems. The eye diagrams are calculated using our receiver model. The eye diagrams are similar to what were obtained in the single channel system, but with more amplitude jitter.

In our model of the Tyco-CRZ system, we observe somewhat more degradation in channel 4 than in channel 2 or 6. This increased degradation is due to low average dispersion in every map period along the line, which increases the nonlinear interchannel interactions. A similar trend is not visible in [1] and [2], perhaps because these experiments used orthogonal polarizations in neighboring channels.

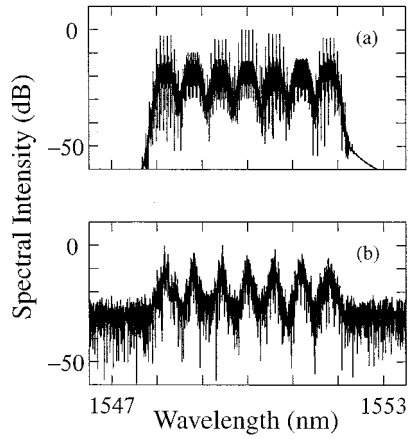

Fig. 9. Evolution of the (a) input and (b) output spectral intensity in the Tyco-CRZ system.

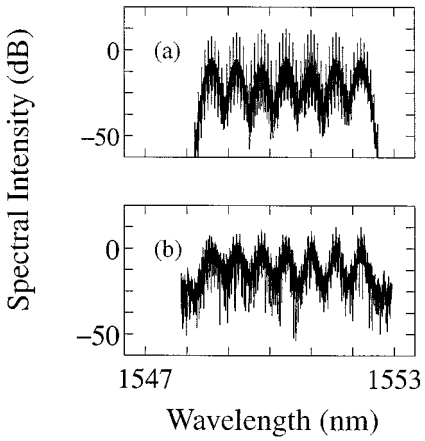

Fig. 10. Evolution of the (a) input and (b) output spectral intensity in the CNET-CRZ system.

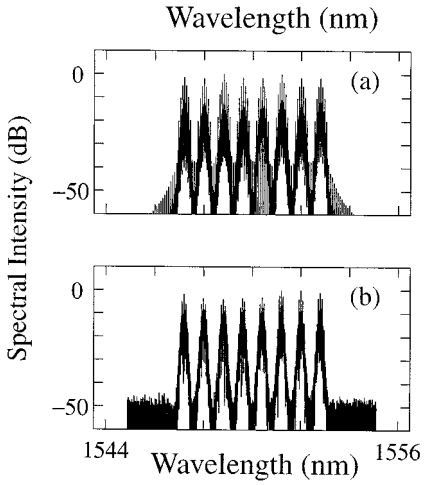

Fig. 11. Evolution of the (a) input and (b) output spectral intensity in the KDD-RZ system.

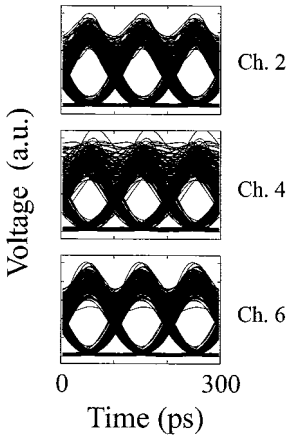

Fig. 12. Eye diagrams of three channels in the 7 × 10 Gb/s Tyco-CRZ WDM system.

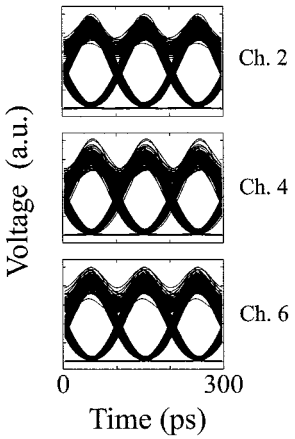

Fig. 13. Eye diagrams of three channels in the 7 × 10 Gb/s CNET-DMS WDM system.

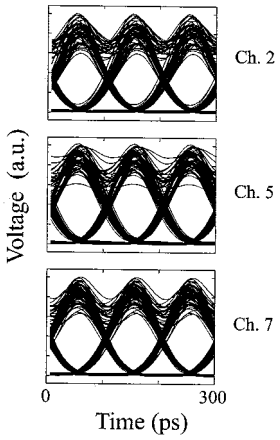

Fig. 14. Eye diagrams of three channels in the 8 × 10 Gb/s KDD-RZ WDM system.

Although we do not show detailed plots of the pulse dynamics here, we have verified that the pulse dynamics is not visibly changed by the interchannel interactions.

We conclude that wavelength division multiplexing degrades the eye diagrams in our three model systems, but it does not change their quasi-linear behavior.

VI. Conclusion

There has been a long debate in the optical fiber communications community over whether it would be preferable to use an NRZ format or a soliton format in long-haul systems. In recent years, the NRZ format has evolved into the CRZ format, while the soliton format evolved into the periodically stationary DMS format and, from there, into the nonperiodically stationary or quasi-linear DMS format. It is our view that the soliton and nonsoliton formats have effectively converged.

In this paper, we compared three systems that exemplify modern-day CRZ, DMS, and RZ systems. We did so by creating computer models that reproduce the essential features of all three systems. We found that the pulse dynamics is dominated by the initial chirp of the pulses and the linear dispersion in the transmission line. We also found that the spread in the electronic eye diagrams is dominated by spontaneous-signal beat noise. This behavior is typical for linear systems. At the same time, we also found that nonlinearity plays an important role in all three systems and must be properly mitigated in order for the typically linear behavior just mentioned to manifest itself. We refer to these systems as quasi-linear to indicate that the pulse dynamics and eye diagrams in these systems resemble those in linear systems, although the nonlinearity plays an important role. These systems resemble each other far more closely than any of them resembles the periodically stationary DMS systems of Suzuki *et al.* [9] or Jacob *et al.* [10].

References

[1] N. S. Bergano, C. R. Davidson, M. Ma, A. N. Pilipetskii, S. G. Evangelides, H. D. Kidorf, J. M. Darcie, E. A. Golovchenko, K. Rottwitt, P. C. Corbett, R. Menges, M. A. Mills, B. Pedersen, D. Peckham, A. A. Abramov, and A. M. Vengsarkar, "320 Gb/s WDM transmission (64 × 5 Gb/s) over 7,200 km using large mode fiber spans and chirped return-to-zero signals," in *Proc. OFC'98*, San Jose, CA, Feb. 1998, PD12.

[2] N. S. Bergano, C. R. Davidson, C. J. Chen, B. Pedersen, M. A. Mills, N. Ramanujam, A. B. Kidorf, H. D. Puc, M. D. Levonas, and H. Abdelkader, "640 Gb/s transmission of sixty-four 10 Gb/s WDM channels over 7,200 km with 0.33 (bits/s)/hz spectral efficiency," in *Proc. OFC'99*, San Diego, CA, Feb. 1999, PD2.

[3] F. Favre, D. Le Guen, M. L. Moulinard, M. Henry, and T. Georges, "320 Gbit/s soliton WDM transmission over 1300 km with 100 km dispersion-compensated spans of standard fiber," *Electron. Lett.*, vol. 33, pp. 2135–2136, Dec. 1997.

[4] D. Le Guen, F. Favre, M. L. Moulinard, M. Henry, G. Michaud, L. Mac, F. Devaux, B. Charbonnier, and T. Georges, "200 GBit/s 100 km-span soliton WDM transmission over 1000 km of standard fiber with dispersion compensation and pre-chirping," in *Proc. OFC'98*, San Jose, CA, Feb. 1998, PD17.

[5] D. Le Guen, S. D. Burgo, M. L. Moulinard, D. Grot, M. Henry, F. Favre, and T. Georges, "Narrow band 1.02 Tbit/s (51 × 20 Gbit/s) soliton DWDM transmission over 1000 km of standard fiber with 100 km amplifier spans," in *Proc. OFC'99*, San Diego, CA, Feb. 1999, PD4.

[6] H. Taga, N. Edagawa, M. Suzuki, N. Takeda, K. Imai, S. Yamamoto, and S. Akiba, "213 Gbit/s (20 × 10.66 Gbit/s), over 9000 km transmission experiment using periodic dispersion slope compensator," in *Proc. OFC'98*, San Jose, CA, February 1998, PD13.

[7] H. Taga, M. Suzuki, N. Edagawa, N. Takeda, K. Imai, S. Yamamoto, and S. Akiba, "20 WDM 10.66 GBit/s transmission experiment over 9000 km using periodic dispersion slope compensation," *Electron. Lett.*, vol. 34, pp. 476–478, Mar. 1998.

[8] H. Taga, M. Suzuki, N. Edagawa, S. Yamamoto, and S. Akiba, "Long-distance WDM transmission experiments using the dispersion slope compensator," *J. Quantum Electron.*, vol. 34, pp. 2055–2063, Nov. 1998.

[9] M. Suzuki, I. Morita, N. Edagawa, S. Yamamoto, H. Taga, and S. Akiba, "Reduction of Gordon-Haus timing jitter by periodic dispersion compensation in soliton transmission," *Electron. Lett.*, vol. 31, pp. 2027–2029, Nov. 1995.

[10] J. M. Jacob and G. M. Carter, "Error-free transmission of dispersion-managed solitons at 10 Gbit/s over 24 500 km without frequency sliding," *Electron. Lett.*, vol. 33, pp. 1128–1129, June 1997.

[11] M. I. Hayee and A. E. Willner, "Pre- and post-compensation of dispersion and nonlinearities in 10-Gb/s WDM systems," *IEEE Photon. Technol. Lett.*, vol. 9, pp. 1271–1273, Sept. 1997.

[12] L. Ding, E. A. Golovchenko, A. N. Pilipetskii, C. R. Menyuk, and P. K. Wai, "Modulated NRZ signal transmission in dispersion maps," in *System Technologies*, A. E. Willner and C. R. Menyuk, Eds. Washington, DC: Opt. Soc. Amer., 1997, vol. 12, pp. 204–206.

[13] R.-M. Mu and C. R. Menyuk, "Symmetric slope compensation in a long haul WDM system using the CRZ format," *IEEE Photon. Technol. Lett.*, vol. 13, pp. 797–799, Aug. 2001.

[14] T. Yu, "Optimal Pulse Formats in Optical Fiber Communications Systems," Ph.D. dissertation, Univ. Maryland Baltimore County, 2000.

[15] R.-M. Mu, "Comparison of the Chirped Return-to-Zero and Dispersion Managed Soliton Modulation Formats in Wavelength Division Multiplexed Systems," Ph.D. dissertation, University of Maryland Baltimore County, Baltimore, MD, 2001.

[16] R.-M. Mu, T. Yu, V. S. Grigoryan, and C. R. Menyuk, "Dynamics of chirped return-to-zero format," *J. Lightwave Technol.*, vol. 20, pp. 47–57, Jan. 2002.

[17] R.-M. Mu, V. S. Grigoryan, C. R. Menyuk, G. M. Carter, and J. M. Jacob, "Comparison of theory and experiment for dispersion-managed solitons in a recirculating fiber loop," *IEEE J. Select. Topics Quantum Electron.*, vol. 6, pp. 248–257, Mar./Apr. 2000.

[18] C. R. Menyuk, "Application of multiple length scale methods to the study of optical fiber transmission," *J. Eng. Math.*, vol. 36, no. 6, pp. 113–136, 1999.

[19] R.-M. Mu, V. S. Grigoryan, C. R. Menyuk, E. A. Golovchenko, and A. N. Pilipetskii, "Timing jitter reduction in a dispersion-managed soliton system," *Opt. Lett.*, vol. 23, no. 12, pp. 930–932, 1998.

[20] T. Tsuritani, N. Takeda, A. Agata, I. Morita, H. Yamauchi, N. Edagawa, and M. Suzuki, "1 Tbit/s (100×10.7 Gbit/s) transoceanic transmission using 30 nm-wide broadband optical repeaters with $A_{\rm eff}$ -enlarged positive dispersion fiber and slope-compensation DCF," in *Proc. ECOC'99*, Nice, France, Oct. 1999, PDII-8.

[21] T. Yu and C. R. Menyuk, "RZ and NRZ signal propagation in optical fiber transmission systems," in *Proc. OSA Annu. Meet.*, Baltimore, MD, Oct. 1998, ThQ4.

[22] T. Yu, W. M. Reimer, V. S. Grigoryan, and C. R. Menyuk, "A mean field approach to WDM simulations," *IEEE Photon. Technol. Lett.*, vol. 12, pp. 443–445, Apr. 2000.

[23] N. S. Bergano and C. R. Davidson, "Wavelength division multiplexing in long-haul transmission systems," *J. Lightwave Technol.*, vol. 14, pp. 1299–1308, June 1996.

[24] Y. Sun, J. W. Sulhoff, A. K. Srivastava, J. L. Zyskind, T. A. Strasser, J. R. Pedrazzini, C. Wolf, J. Zhou, J. B. Judkins, R. P. Espindola, and A. M. Vengsarkar, "80 nm ultra-wideband erbium-doped silica fiber amplifer," *Electron. Lett.*, vol. 33, pp. 1965–1967, Nov. 1997.

R.-M. Mu, photograph and biography not available at the time of publication.

C. R. Menyuk (SM'88–F'98) was born March 26, 1954. He received the B.S. and M.S. degrees from the Massachusetts Institute of Technology, Cambridge, in 1976 and the Ph.D. degree from the University of California, Los Angeles, in 1981.

He has worked as a Research Associate at the University of Maryland, College Park, and at Science Applications International Corporation, McLean, VA. In 1986, he became an Associate Professor in the Department of Electrical Engineering at the University of Baltimore Count (UMBC), Baltimore, and he was the founding member of the department. In 1993, he was promoted to Professor. He has been on partial leave from UMBC since 1996. From 1996 to 2001, he worked part-time for the Department of Defense (DoD), codirecting the Optical Networking Program at the DoD Laboratory for Telecommunications Sciences in Adelphi, MD, from 1999 to 2001. In August, 2001, he left DoD and became Chief Scientist at PhotonEx Corporation. For the last 15 years, his primary research area has been theoretical and computational studies of fiber-optic communications. He has authored or coauthored more than 140 archival journal publications as well as numerous other publications and presentations. He has also edited two books. The equations and algorithms that he and his research group at UMBC have developed to model optical fiber transmission systems are used extensively in the telecommunications industry.

Dr. Menyuk is a Fellow of the Optical Society of America (OSA) and a member of the Society for Industrial and Applied Mathematics and the American Physical Society. He is a former UMBC Presidential Research Professor.